A Miocene tectonic inversion in the Ionian Sea (central Mediterranean): Evidence from multichannel seismic data

Flora Gallais, Marc-André M-A Gutscher, David Graindorge, Nicolas Chamot-Rooke, D. Klaeschen

A Miocene tectonic inversion in the Ionian Sea (central Mediterranean): Evidence from multichannel seismic data

Flora Gallais,[1,2] Marc-André Gutscher,[1,2] David Graindorge,[1,2] Nicolas Chamot-Rooke,[3] and Dirk Klaeschen[4]

Received 3 May 2011; revised 22 September 2011; accepted 26 September 2011; published 23 December 2011.

[1] It is widely accepted that the Central and Eastern Mediterranean are remnants of the Neo-Tethys. However, the orientation and timing of spreading of this domain remain controversial. Here, we present time migrated and pre-stack depth migrated NW-SE oriented Archimede (1997) lines together with the PrisMed01 (1993) profile to constrain the evolution of the Ionian basin. Our interpretation allows us to identify a large-scale set of SW-NE striking reverse faults beneath the Ionian Abyssal Plain. These primarily NW vergent faults have a characteristic spacing of 10 to 20 km and a dip ranging from 60 to 65°. Following very recent paleogeographic reconstructions, we propose that the set of N°55 features initially formed as normal faults during NW-SE trending seafloor spreading of the Ionian basin after its late Triassic-early Jurassic rifting. Based on geometric comparisons with the intraplate deformation observed beneath the Central Indian Ocean, we show that the inherited oceanic normal faults were reactivated under compression as reverse faults. Well-developed Tortonian syntectonic basins developed NW of the major faults and the base of the Messinian evaporites (Mobile Unit) is slightly folded by the activity of the faults. We show that 3–4 km of total shortening occurs over a 80 km wide area beneath the Ionian Abyssal Plain, resulting in a bulk shortening of 3.5–5%. We propose a link between the Tortonian-early Messinian inversion of the fault pattern and a plate tectonic reorganization prior to the main phase of back-arc opening of the Tyrrhenian domain.

Citation: Gallais, F., M.-A. Gutscher, D. Graindorge, N. Chamot-Rooke, and D. Klaeschen (2011), A Miocene tectonic inversion in the Ionian Sea (central Mediterranean): Evidence from multichannel seismic data, *J. Geophys. Res.*, *116*, B12108, doi:10.1029/2011JB008505.

1. Introduction and Geological Setting

[2] The Central Mediterranean area is characterized by wide-spread pattern of weak to moderate seismicity, indicating a region undergoing diffuse deformation (Figure 1) [*Chiarabba et al.*, 2005; *Pondrelli et al.*, 2006]. The seismotectonic setting of this region is the consequence of the long-term African-Eurasian convergence, which is one of the primary controls on the deformation in the region [*Di Bucci et al.*, 2010]. Geodetic studies conclude that the overall Nubia-Eurasia convergence continues at very slow rates, ranging from 6 mm/yr near Greece oriented N to NNW to 5–7 mm/yr near Sicily oriented NNW to NW [*DeMets et al.*, 1994; *Hollenstein et al.*, 2003; *Serpelloni et al.*, 2007; *D'Agostino et al.*, 2008]. Regional Global Positioning System (GPS) measurements can only be explained by the presence of a mosaic of microplates in the Central Mediterranean, which move almost independently [*Serpelloni et al.*, 2007; *D'Agostino et al.*, 2008, 2011].

[3] Within the Ionian Sea, the Mediterranean Ridge and the Calabrian prism are interpreted as two large accretionary complexes, which formed in response to the subduction of the African plate beneath Eurasia (s.l.) (Figure 1) [*Finetti*, 1982; *Reston et al.*, 2002; *Chamot-Rooke et al.*, 2005; *Minelli and Faccenna*, 2010]. The deep Ionian Abyssal Plain (IAP) is the foreland of the Calabrian prism to the NW and of the western Mediterranean Ridge to the NE (Figure 1). It is a deep triangular basin roughly 5000 km^2 in area [*Hieke et al.*, 2003], well-defined by the 4000 m depth isobath and bounded to the South by the Medina Seamounts (Figure 2). The Victor Hensen Seahill 2 (VHS 2) and the Victor Hensen Seahill (VHS) rise above the South-East of the IAP [*Hieke*, 1978; *Hieke and Wanninger*, 1985; *Hieke et al.*, 2003]. The VHS is interpreted as a roughly 10 km long and 2 km wide SW-NE elongated tectonic structure [*Hieke and Wanninger*, 1985; *Hieke et al.*, 2006]. North-West

[1]Domaines Océaniques, Université Européenne de Bretagne, Plouzané, France.
[2]Domaines Océaniques, UMR 6538, Université de Brest, CNRS, Institut Universitaire Européen de la Mer, Plouzané, France.
[3]Laboratoire de Géologie, Ecole Normale Supérieure, Paris, France.
[4]Leibniz Institute of Marine Sciences at University of Kiel (IFM-GEOMAR), Kiel, Germany.

0148-0227/11/2011JB008505

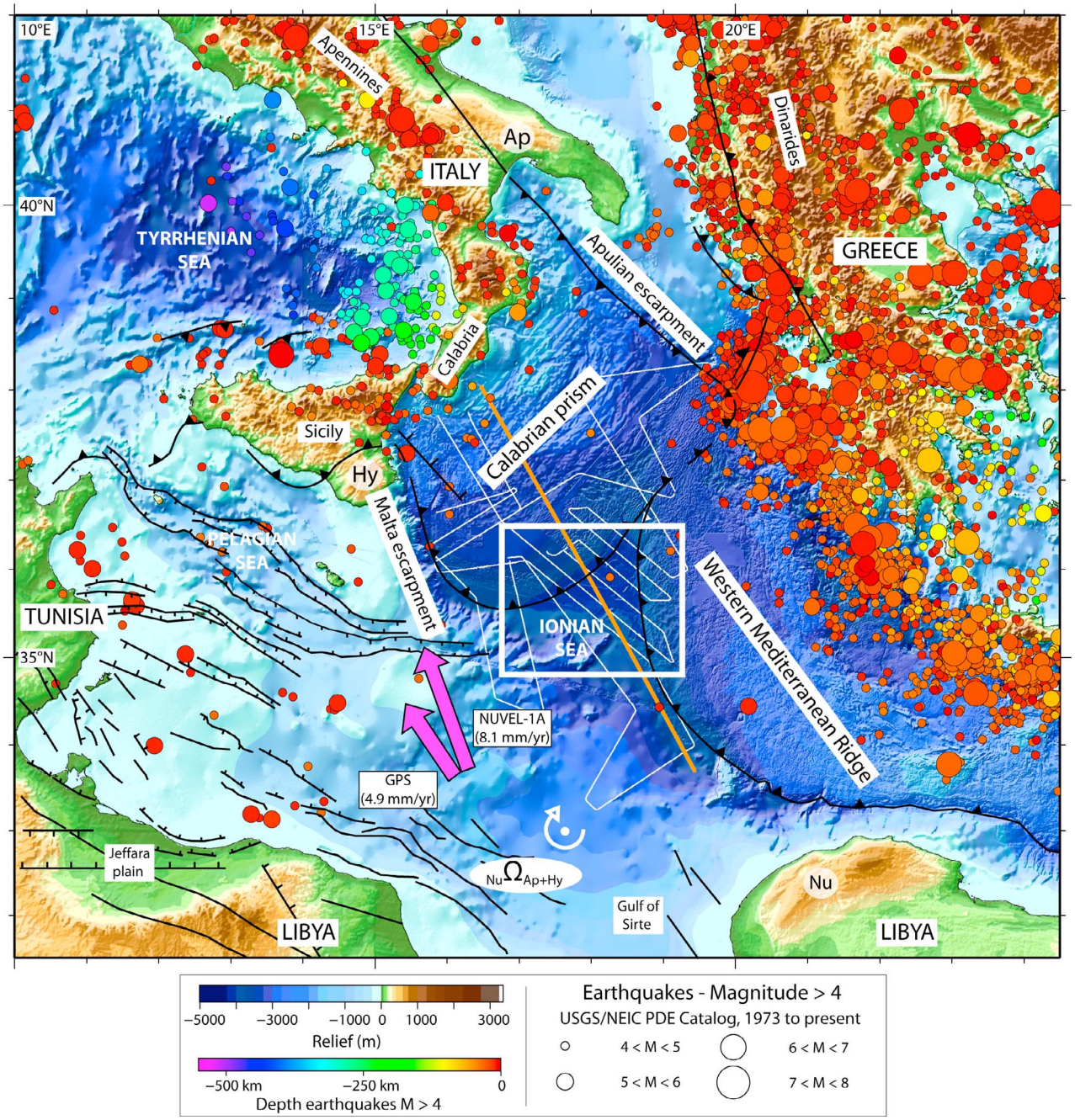

Figure 1. Seismotectonic map of the Central Mediterranean area (topography and bathymetry are from GEBCO 1 min data set and Medimap Group Bathymetry compilation [*Loubrieu et al.*, 2007]). Black lines show major fault systems (modified from the Geodynamic Map of the Mediterranean (Commission for the Geological Map of the World, http://ccgm.free.fr) and offshore regions beneath the Pelagian Sea from *Raulin et al.* [2011]). Earthquake hypocenters are from the National Earthquake Information Center (NEIC) catalog (http://neic.usgs.gov). Magenta arrows show the convergence between Africa and Eurasia according to the NUVEL-1A model [*DeMets et al.*, 1994] and the GPS pole of rotation proposed by *D'Agostino et al.* [2008]. White point surrounded by curved white arrow shows the Eulerian pole of rotation $_{Nu}\Omega_{Ap+Hy}$, which indicates the poles of rotation relative to Nubia (Nu), obtained considering Apulia (Ap) and the Hyblean Plateau (Hy) as a single microplate [*D'Agostino et al.*, 2008]. Thin white lines show the position of the Archimede seismic cruise (1997, R/V Le Nadir), and thin orange line shows the position of the line PrisMed01 acquired during the PrisMed cruise (1993, R/V Le Nadir). Study area (shown in Figures 2 and 6) is indicated by the white square.

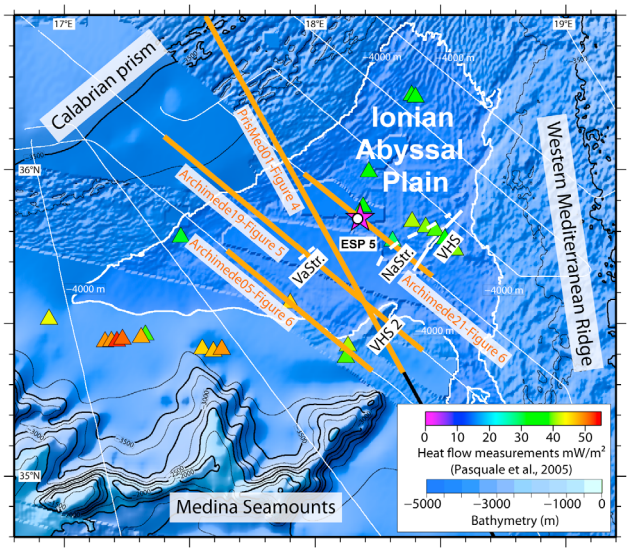

Figure 2. Bathymetry and location map: The Ionian Abyssal Plain is roughly defined by the 4000 m depth isobaths (thick white contour). Triangles indicate heat flow values [*Pasquale et al.*, 2005]. White circle indicates the position of the DSDP Site 374 [*Hsü et al.*, 1978], and magenta star indicates the position of the ESP [*de Voogd et al.*, 1992]. The main structural features are indicated as follows: NaStr., Nathalie Structure; VaStr, Valvidia Structure; VHS, Victor Hensen Seahill; VHS2, Victor Hensen Seahill 2 (nomenclature from *Hieke et al.* [2003]). Thick orange lines indicate the profiles shown in Figures 4–6.

of the VHS, three SW/NE subbottom structures were imaged: the Nathalie Structure (NaStr.), the Valvidia Structure (VaStr.) and the Victor Hensen Seahill Structure (VHStr.), which was interpreted as the SW-NE oriented subbottom continuation of the Victor Hensen Seahill [*Finetti*, 1982; *Hieke et al.*, 2003] (Figure 2). In situ heat flow measurements show very low values beneath the Ionian Abyssal Plain (30 to 40 mW/m^2) (Figure 2) [*Pasquale et al.*, 2005]. South-West of the IAP, close to the Medina Seamounts, measured heat flow values increase (values range from 45 to 55 mW/m^2) (Figure 2) [*Pasquale et al.*, 2005].

[4] Numerous seismic reflection and refraction studies have imaged the IAP and the adjacent crystalline basement [*Finetti*, 1982; *Makris et al.*, 1986; *de Voogd et al.*, 1992; *Sioni*, 1996; *Catalano et al.*, 2001; *Chamot-Rooke et al.*, 2005; *Hieke et al.*, 2003]. There is an ongoing debate regarding the nature of the crust under-lying the Ionian Abyssal Plain. Some authors consider that the high-amplitude layered band seismic signature near the base of the crust differs from other old oceanic reflection images (e.g., eastern Atlantic Ocean) [*Cernobori et al.*, 1996]. Other authors invoke the structural continuity between the Medina Seamounts (known to be of continental affinity [*Finetti*, 1982; *Hieke and Wanninger*, 1985]) and the Victor Hensen Seahill as an argument in favor of a thinned continental crust underlying the IAP [*Hieke et al.*, 2003]. However, all the Expanding Spread Profile (ESP) results conclude that the Ionian Abyssal Plain is floored by a more than 5 km thick Meso-Cenozoic sedimentary cover, deposited over a thin crust [*Makris et al.*, 1986; *de Voogd et al.*, 1992; *Le Meur*, 1997]. These refraction results show a typical oceanic velocity gradient [*Makris et al.*, 1986; *de Voogd et al.*, 1992; *Le Meur*, 1997] and a 7 to 9 km crustal thickness [*Le Meur*, 1997; *Chamot-Rooke et al.*, 2005], compatible with the world-wide compilation of typical oceanic thicknesses [*White et al.*, 1992]. The depth of the Moho is 16 to 18 km beneath the IAP and the mantle is characterized by a high refraction velocity of 8.5 km/s [*de Voogd et al.*, 1992].

[5] Paleogeographic reconstructions of the Central and Eastern Mediterranean basins are based on geological data from the surrounding areas of the Mediterranean Sea (e.g., in Sicily, Tunisia, Western Desert, Syria and Oman), and on the geometry of the paleo-passive and transform margins (focused mainly on the Levant margin) (see references given by *Stampfli et al.* [1991], *Ricou* [1994], *Garfunkel* [1998], *Golonka* [2004], *Stampfli and Borel* [2004], *Guiraud et al.* [2005], *Frizon de Lamotte et al.* [2011], *Raulin et al.* [2011], and *Schettino and Turco* [2011]). These paleogeographic studies all conclude that the Central and Eastern Mediterranean basins corresponds to a relic of the Neo-Tethys [*Şengör*, 1979]. But it is interpreted either as the easternmost continuity of the Neo-Tethys [*Stampfli et al.*, 1991; *Stampfli and Borel*, 2004] or as a secondary southern branch connected to it [*Dercourt et al.*, 1986; *Ricou*, 1994; *Garfunkel*, 1998; *Frizon de Lamotte et al.*, 2011]. In the Central Mediterranean, the geometry and timing of spreading of the Ionian basin is controversial [*Stampfli et al.*, 1991; *Ricou*, 1994; *Handy et al.*, 2010; *Frizon de Lamotte et al.*, 2011].

[6] Some authors proposed that during the Cretaceous, the 30° counter-clockwise rotation of Apulia with respect to Africa led to the opening of the Central and Eastern Mediterranean [*Dercourt et al.*, 1986; *Golonka*, 2004]. This rotation was interpreted to be coeval with the main phase of opening, deepening and widening of the Ionian basin [*Chamot-Rooke et al.*, 2005]. These authors proposed that the Ionian basin ceased its spreading in late Cretaceous time, contemporary with the Alpine collision with Eurasia, North of Apulia, as a consequence of the northward motion of Africa [*Dercourt et al.*, 1986; *Golonka*, 2004].

[7] Based on the presence of Permian marine basins from Sicily to Syria, many workers concluded that the Neo-Tethys opened synchronously in the late Paleozoic across the entire Eastern Mediterranean [*Robertson et al.*, 1991; *Stampfli et al.*, 1991; *Stampfli and Borel*, 2004]. Within this framework, the Ionian basin may have formed during the late Paleozoic, either in response to rifting process [*Stampfli et al.*, 1991; *Stampfli and Borel*, 2004] or to back-arc extension as a result of a southward-dipping subduction zone [*Şengör*, 1979; *Şengör et al.*, 1984; *Schettino and Turco*, 2011]. The cessation of the spreading center in the basin is interpreted to occur during the late Triassic, associated with the presence of the first important rift structures in Italy [*Schettino and Turco*, 2011].

[8] Very recently, it was suggested that the Eastern Mediterranean corresponds to a secondary branch of the Neo-Tethys, that opened NW-SE following the late Triassic-early Jurassic rifting [*Frizon de Lamotte et al.*, 2011; *Raulin et al.*, 2011]. In the easternmost Mediterranean region, the presence of Triassic-Jurassic NE-SW veering to E-W normal faults led workers to interpret the Levant margin and the

Western Desert as passive margins, in direct relation with the Neo-Tethyan rifting [*Garfunkel*, 1998; *Guiraud et al.*, 2005; *Frizon de Lamotte et al.*, 2011]. In southern Tunisia, the Jeffara basin (Figure 1) is a very proximal margin of the Ionian basin, where similar late-Triassic-early Jurassic extensional deformation is observed [*Frizon de Lamotte et al.*, 2011; *Raulin et al.*, 2011]. This tectonic model features the Central Mediterranean opening in a NW-SE direction, during the late Triassic-early Jurassic [*Frizon de Lamotte et al.*, 2011; *Raulin et al.*, 2011]. These authors further suggest that the Malta escarpment (Figure 1) is a NW-SE oriented transform fault bounding this Neo-Tethyan domain toward the West [*Frizon de Lamotte et al.*, 2011].

[9] Although the post-Oligocene evolution of the Mediterranean (including the Ionian basin) is well understood in the framework of a back-arc opening above a retreating subduction zone [*Faccenna et al.*, 2001; *Rosenbaum et al.*, 2002], its prior paleogeographic evolution is still controversial, in particular the geometry of rifting and spreading in the Ionian basin [*Dercourt et al.*, 1986; *Robertson et al.*, 1991; *Stampfli et al.*, 1991; *Garfunkel*, 1998; *Golonka*, 2004; *Guiraud et al.*, 2005; *Handy et al.*, 2010; *Frizon de Lamotte et al.*, 2011; *Raulin et al.*, 2011; *Schettino and Turco*, 2011]. To address this question, we present the most relevant time-migrated lines of the Archimede multichannel seismic survey (1997, R/V Le Nadir) and the first pre-stack depth migrated profiles crossing the Ionian Abyssal Plain: the Archimede 19 line and the PrisMed01 line, acquired during the PrisMed survey (1993, R/V Le Nadir). We first present the data set used to study the Ionian Abyssal Plain and the processing sequence applied, including details on the sophisticated pre-stack depth migration. In a second part we propose a stratigraphy of the sediments deposited beneath the Ionian Abyssal Plain, based on seismic correlations and new knowledge of the Messinian sediments in the Mediterranean basins. We thus focus on the deformation affecting the sediments and discuss the possible link with the Messinian deposition and the subbottom structures and structural basement highs present beneath the Ionian Abyssal Plain. An interpretation of the origin of these structures and timing of their reactivation and the kinematic implications is then be proposed in the framework of the evolution of the IAP.

2. Multichannel Seismic Reflection Data and Processing

2.1. The 96-Channel Archimede Survey and Processing of the Data

[10] The Archimede survey was conducted from 9 to 24 April 1997 onboard R/V Le Nadir (Figure 1). The objectives were to image the deep structures of the Mediterranean Ridge and the Calabrian wedge and the fracturing of the basement beneath the Ionian Abyssal Plain. The Archimede seismic data set consists of 35 seismic reflection profiles with a total length of 2500 km. Data were recorded by a 96-channel 2.4 km long streamer. The shot spacing of 50 m and the 25 m between each hydrophone provide a 24 fold coverage, with a CMP spacing of 12.5 m. The seismic data were acquired with 4 ms sampling rate (250 Hz). The source was an air gun array consisting of ten air guns for a total volume of 1220 cu.in, operating in a single-bubble mode [*Avedik et al.*, 1996] and placed at a depth of 20 m. In contrast to tuned arrays, this kind of system exploits the strong energy contained in the first bubble pulse delaying the firing of guns as a function of their volume in order to synchronize the output of the guns with respect to this first pulse [*Avedik et al.*, 1996]. The single-bubble method generates a powerful low frequency signal (10 to 15 Hz), which allows a better penetration of signal to image the deep structures [*Avedik et al.*, 1996; *Bartolome et al.*, 2005].

[11] During data processing, with the GeoVecteur Software© developed by CGG (Compagnie Générale de Géophysique), particular attention was paid to improve the continuity of the deep reflectors beneath the IAP. A 6/8/55/65 passband filter and a 49/50/51 notch filter, as well as a spherical divergence correction were generally applied after a spectral analysis of the near trace of the profiles. Before stacking, a predictive deconvolution was applied to the signal with a typical window of 5 s TWT. This deconvolution attempts to predict and remove repetitions in the recorded seismograms, it also acts like an anti-multiple on many profiles [*Yilmaz*, 1987]. For each Archimede line, a velocity analysis based on a semblance computation was performed each 300 Common Mid Point (CMP) (equal to 3.75 km) to constrain the lateral velocity variations. The velocity libraries obtained after interactive picking of these semblances are used to compute a normal move out (NMO) correction. The NMO corrected CMP gather were stacked in order to increase the signal/noise ratio. To correct numerous diffractions, in particular in the deformed Messinian units in the wedges, different migration velocities were tested. After some tests, we conclude that the diffractions are well corrected with a 2900 m/s constant velocity Kirchhoff migration [*Hubral*, 1977], representative of the average of the root-mean square velocities in the full seismic section. This sequence was applied to entire Archimede data set, and was chosen for its efficiency as it considerably improves the strength and the continuity of the deep reflectors beneath the IAP.

2.2. The 96-Channel PrisMed Cruise and Processing of the Data

[12] The PrisMed seismic survey was conducted from February 27 to March 27 1993 and acquired 3600 km of seismic lines. Here, we will present only part of the PrisMed01 profile, acquired from the Calabrian prism to the Ionian Abyssal Plain (Figure 1). The PrisMed01 line and the Archimede 19 line were processed using the Pre-Stack Depth Migration (PSDM) technique. The PrisMed seismic data were acquired with an AMG 96-channel streamer. The SERCEL 358 acquisition laboratory registered data with a sample rate of 4 ms. Six air guns were immersed at a depth of 10 to 15 m. The signal was recorded with a 2.4 km long 96-channel streamer. The shotpoint interval of 19.4 s corresponding to a shot interval of 50 m yields a 24-fold coverage, at a CMP spacing of 12.5 m.

[13] Before performing depth-focusing analysis during Pre-Stack Depth Migration, several processing steps were applied with the commercial processing software OMEGA2© from WesternGeco to the raw seismic data (frequency filter, spherical divergence correction, shot gather consistent deconvolution

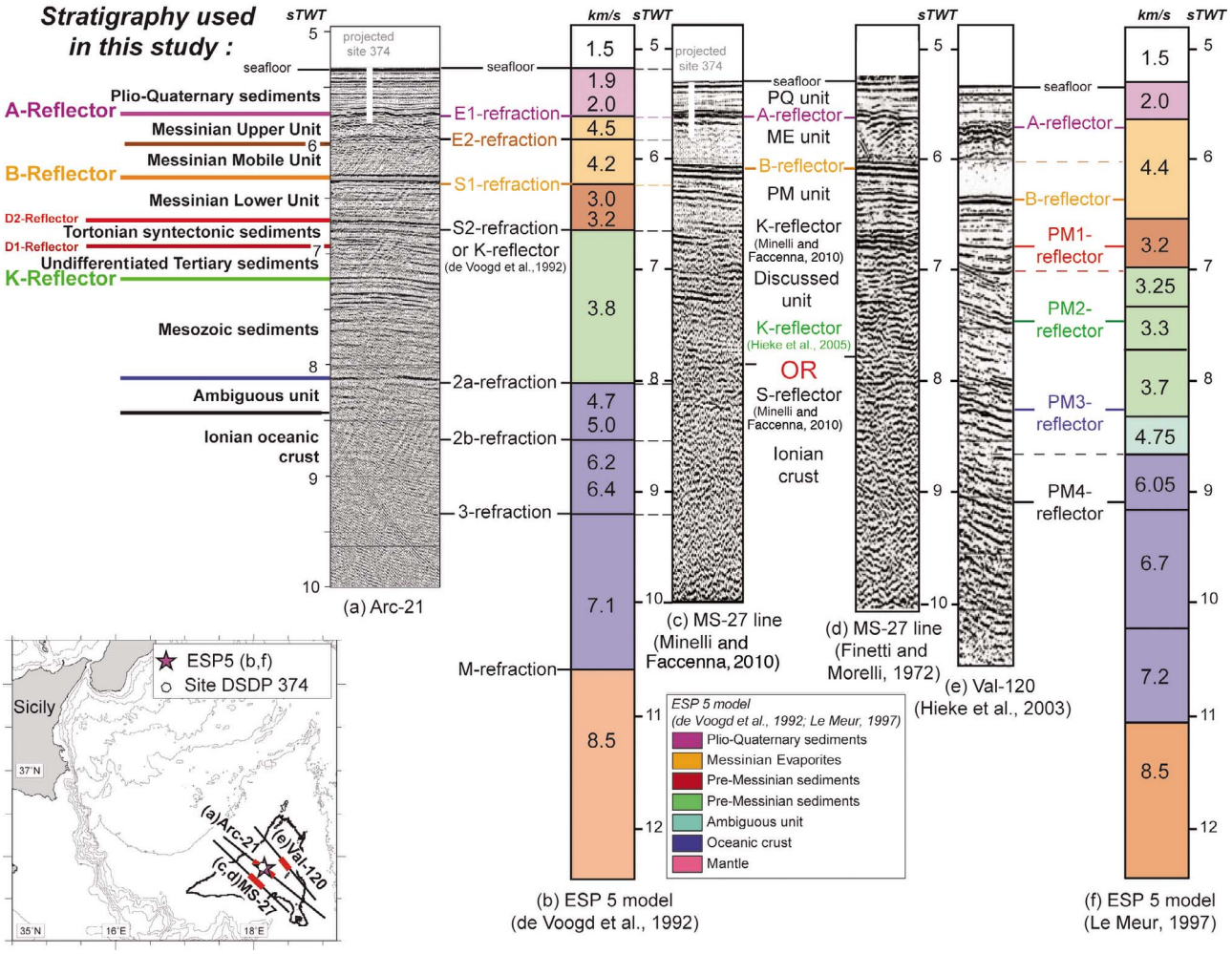

Figure 3. Stratigraphy beneath the Ionian Abyssal Plain, identified by published multichannel seismic reflection profiles from (c) *Minelli and Faccenna* [2010], (d) *Finetti and Morelli* [1972], and (e) *Hieke et al.* [2003], correlated with the ESP 5 velocity model from (b) *de Voogd et al.* [1992] and (f) *Le Meur* [1997]. Note that the stratigraphy shown is the original interpretation and these are presented for this study at the same vertical scale in s TWT. (a) Example of the line Archimede 21 (Arc-21), with stratigraphy and main reflectors identified in this study (the D1-reflector and D2-reflector defined by *Sioni* [1996]). PQ, Plio-Quaternary unit; ME, Messinian unit; PM, Pre-Messinian.

with 36 ms prediction lag and 200 ms operator length for the shallow sediment structures and 72 ms prediction lag and 600 ms operator length for the deeper structures, respectively). Special attention was paid to the water bottom multiple attenuation. A combination of Wave-Equation demultiple (modeling, gather-match, subtraction) and Frequency-Wave number (FK) demultiple (NMO over correction, filter, inverse NMO) gave the best result. The Archimede 19 and PrisMed01 profiles were then processed, with the commercial Kirchhoff migration package KirPack (SIRIUS, GX Technology), to perform a Pre-Stack Depth Migration (PSDM). The PSDM not only produces a section in depth, but also corrects for the refraction and bending of the rays at velocity interfaces and gradients [*Hubral*, 1977]. A combination of iterative PSDM and focusing analyses each 200 Common Depth-Point (CDP) yielded a geologically plausible internal velocity model for the entire Archimede 19 and PrisMed01 lines. Both profiles underwent a series of 5 iterative migrations using a velocity model, from the top of the seismic section to the bottom. It is necessary to construct the velocity model layer by layer from top to bottom, as the upper layer velocities affect those determined for deeper units [*Reston et al.*, 1996]. To begin with, the initial water velocity model is estimated for the seismic section, and a first iteration is run. The result is tested and the velocity model is updated adding the presumed uppermost sedimentary layers through depth-focusing error analysis. Then, a second iteration is run, and the procedure is repeated until the entire section from the top to the bottom has been analyzed for velocity. This procedure was repeated five times and the basement velocity was fixed at 6 km/s, according to the results given by the seismic refraction studies [*de Voogd et al.*, 1992]. The PSDM is particularly efficient because the orientation of the Archimede 19 and PrisMed01 profiles (Figure 1)

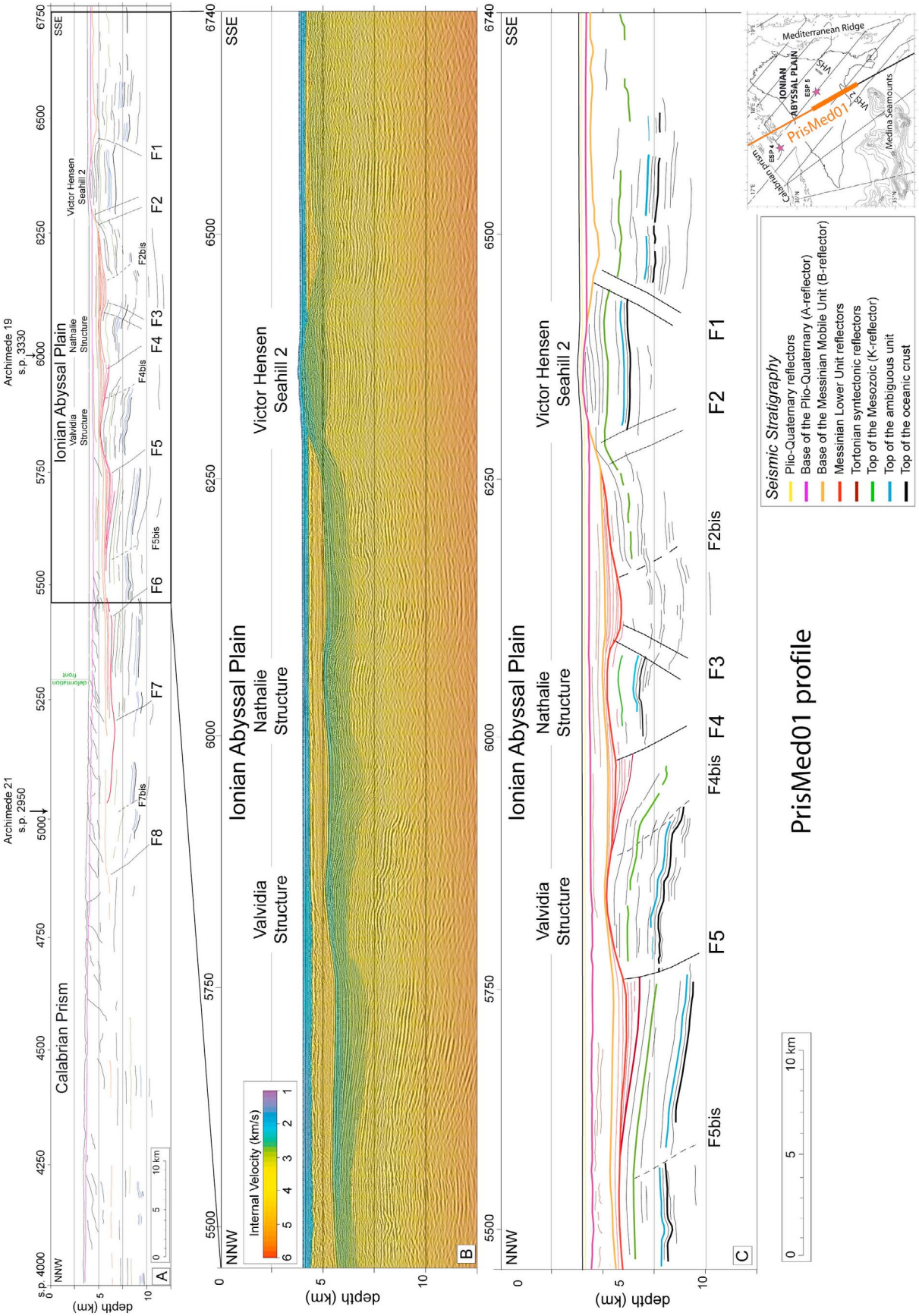
Archimede 19
s.p. 3330
Archimede 21
s.p. 2950
Calabrian Prism
Ionian Abyssal Plain
Valvidia Structure
Nathalie Structure
Victor Hensen
Seahill 2
deformation front
F1
F2
F2bis
F3
F4
F4bis
F5
F5bis
F6
F7
F7bis
F8
NNW
SSE
depth (km)
Internal Velocity (km/s)
PrisMed01 profile
Seismic Stratigraphy
Plio-Quaternary reflectors
Base of the Plio-Quaternary (A-reflector)
Base of the Messinian Mobile Unit (B-reflector)
Messinian Lower Unit reflectors
Tortonian syntectonic reflectors
Top of the Mesozoic (K-reflector)
Top of the ambiguous unit
Top of the oceanic crust
Mediterranean Ridge
IONIAN ABYSSAL PLAIN
Medina Seamounts
Calabrian prism
PrisMed01
ESP 4
ESP 5
VHS1
VHS2
10 km

Figure 4

is orthogonal to the primary structures. The result is an optimized depth section migrated and an interval velocity model which is both detailed and geologically meaningful.

3. Results

3.1. Stratigraphy Beneath the Ionian Abyssal Plain

[14] The sedimentary sequences are particularly well-imaged beneath the Ionian Abyssal Plain. This is a consequence of the powerful source used during the Archimede and PrisMed seismic surveys and the nearly complete lack of deformation affecting the shallow sediments.

[15] The upper seismic unit corresponds to the unconsolidated Plio-Quaternary sediments. On the Archimede and PrisMed01 profiles, the Plio-Quaternary unit is characterized by a velocity gradient of 1.8 to 2 km/s [*de Voogd et al.*, 1992; *Le Meur*, 1997] and by sub-parallel high-frequency and low-amplitude reflectors [*Hieke et al.*, 2003; *Minelli and Faccenna*, 2010] (Figures 3b and 3d). The thickness of these sediments is about 0.4 s TWT (about 400 m) (Figures 3a and 4). They have been drilled at DSDP site 374 (Figure 1), which allowed identification of a 300 m thick layer of Plio-Quaternary (PQ) sediments and a 60 to 80 m thick Pliocene sequence [*Hsü et al.*, 1978], mostly composed of transparent seismic layered turbidites, called "homogenites" [*Hieke*, 1984; *Cita and Rimoldi*, 1997; *Hieke and Werner*, 2000]. At the base of the Plio-Quaternary sequence, the strong continuous high-amplitude reflector corresponds to the A-reflector (Figures 3a and 3c–3e) [*Finetti and Morelli*, 1972] and the E1-horizon (Figure 3b) [*de Voogd et al.*, 1992].

[16] This A-reflector corresponds to the top of the Messinian unit [*Finetti and Morelli*, 1972], except when morphological highs, associated with structural basement highs, are present (e.g., Figure 4 (s.p. 6300 to 6420)). On the Archimede (Figure 3a) and PrisMed01 lines (Figure 4), the Messinian unit is composed of a weakly reflective sequence (about 0.25 s TWT thick), characterized by continuous reflectors, deposited over a reflection-free 0.35 s TWT thick unit. The base of this reflection-free unit is marked by a planar high-amplitude reverse polarity reflector, which corresponds to the B-reflector (Figures 3a and 3d) [*Finetti and Morelli*, 1972] or the S1-horizon (Figure 3b) [*de Voogd et al.*, 1992]. The ESP 5 allows identification of an intra-Messinian reflector (E2-horizon, Figure 3b). Based on the seismic facies, an "Upper Evaporites" unit and a "Lower Evaporites" unit (composed of halite) were already differentiated [*Hsü et al.*, 1978]. The Messinian unit consists of two layers, with a velocity inversion at its base (B-reflector) around 6.27 s TWT or 6.55 s TWT (from 4.5 to 4.2 to 3.0–3.2 km/s), depending on the ESP 5 model chosen (respectively, Figures 3b and 3e) [*de Voogd et al.*, 1992; *Le Meur*, 1997].

[17] Below the B-reflector, a sequence, characterized by a propagation velocity of 3 to 3.2 km/s (Figures 3b and 3e) and by a succession of high-amplitude and low frequency reflectors (Figure 3a) was interpreted as Tortonian in age [*Cernobori et al.*, 1996; *Chamot-Rooke et al.*, 2005]. A Tortonian age has been proposed due to its stratigraphic position related to the previously described "Lower Evaporites" [*Chamot-Rooke et al.*, 2005]. However, a recent Atlas, dealing with seismic markers of the Messinian Salinity Crisis, proposed that a "Messinian trilogy" [*Ryan et al.*, 1973] was deposited in the deep basins of the Western Mediterranean area during the Crisis [*Lofi et al.*, 2011a]. It is based on seismic facies and the geometric relationship of the units with respect to the evaporitic layer [*Lofi et al.*, 2011a], previously called the Lower Evaporites [*Ryan et al.*, 1973; *Hsü et al.*, 1978]. The Messinian sequence is then composed of a Messinian Upper Unit, characterized by a group of parallel and relatively continuous reflections, underlain by a reflection-free seismic facies Messinian Mobile Unit and finally a Messinian Lower Unit [*Lofi et al.*, 2011a]. Based primarily on observations in the deepest part of the Gulf of Lions, the Messinian Lower Unit is described as a group of continuous high-amplitude reflections that onlap the margin [*Lofi et al.*, 2005; *Lofi and Berne*, 2008; *Lofi et al.*, 2011a, 2011b]. These authors do however caution that the extension and the thickness of this Messinian Lower Unit remains poorly known [*Lofi et al.*, 2011a]. On the Algerian margin, the reflectivity of this Messinian Lower Unit is slightly lower than in the Gulf of Lions [*Lofi et al.*, 2011a]. On top of this unit of a planar high-amplitude reflector has been identified and described as the B-reflector in the deep Ionian Abyssal Plain (Figure 3). Based on seismic facies correlation and observation of the B-reflector, we propose adopting this "Messinian trilogy" to the Ionian Abyssal Plain (Figure 3a). In this case, the Messinian Upper Unit and the reflection-free Messinian Mobile Unit lie above the B-reflector and the Messinian Lower Unit below the B-reflector. The base of the Messinian Lower Unit is characterized by a continuous high-amplitude reflector (Figure 3a, D2-reflector [*Sioni*, 1996]; Figure 3e, PM1-reflector [*Hieke et al.*, 2003]).

[18] This reflector corresponds to the top of a syntectonic unit, characterized by a group of high-amplitude low-frequency reflections (Figure 3a). We proposed a Tortonian age for this unit, present in sub-basins beneath the Ionian Abyssal Plain (Figure 4). Below this unit, an undifferentiated Tertiary sequence has been interpreted due to its stratigraphic position compared to the position of the K-reflector. The K-reflector was interpreted as a planar and continuous reflector at a 7.5 s TWT constant depth, corresponding to the top of the Mesozoic sediments (Figure 3a) [*Finetti and Morelli*, 1972] (Figures 3a and 3e, PM2-reflector [*Hieke et al.*, 2003]).

[19] Published interpretations of refraction seismic data (ESP 5) allow identification of the top of the Ionian oceanic crust at 8.1 s TWT depth (about 9.0 km depth), characterized

Figure 4. Zoom on the pre-stack depth migrated PrisMed01 profile (no vertical exaggeration). (a) On the line drawing, see (1) the thin skinned SE vergent thrust faulting caused by the accretion of post-evaporitic (Messinian Mobile Unit) deposits, forming the Calabrian prism (s.p. 5300 (deformation front) to 4000), and (2) the thick skinned (crustal scale) NW vergent reverse faulting (s.p. 4800 to 6400). (b) Portion of the profile PrisMed01 line in depth (with the internal velocity model obtained during depth migration). (c) Line drawing of the extract showing the geometry of the reverse faults, with dips ranging from 60 to 65°. Note the presence of well-developed Tortonian syntectonic basins (dark red reflectors, s.p. 5500 to 5750 and s.p. 5825 to 5900) and their link with the morphologic highs (Nathalie and Valvidia Structures and VHS 2).

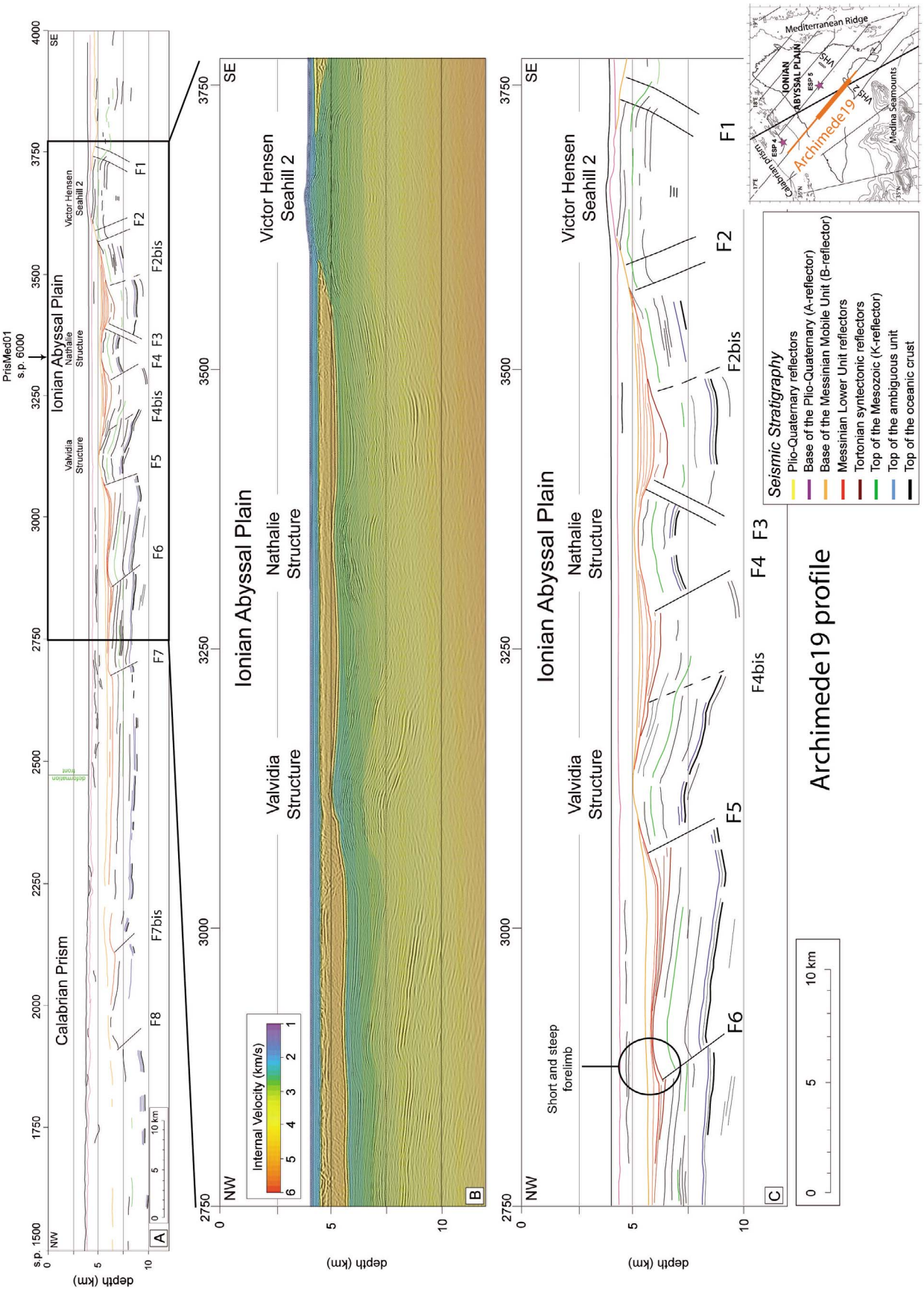
PrisMed01
s.p. 6000
Ionian Abyssal Plain
Nathalie Structure
Valvidia Structure
Victor Hensen Seahill 2
Calabrian Prism
F1
F2
F2bis
F3
F4
F4bis
F5
F6
F7
F7bis
F8
NW
SE
A
B
C
depth (km)
Internal Velocity (km/s)
Short and steep forelimb
Archimede19 profile
Seismic Stratigraphy
Plio-Quaternary reflectors
Base of the Plio-Quaternary (A-reflector)
Base of the Messinian Mobile Unit (B-reflector)
Messinian Lower Unit reflectors
Tortonian syntectonic reflectors
Top of the Mesozoic (K-reflector)
Top of the ambiguous unit
Top of the oceanic crust
Mediterranean Ridge
IONIAN ABYSSAL PLAIN
Medina Seamounts
Archimede19
10 km

Figure 5

by a velocity gradient of 4.7 to 5 km/s [*de Voogd et al.*, 1992] (Figure 3b). This 8.3 km thick crust is interpreted to be oceanic, due to the typical velocity gradient of an oceanic crust [*White et al.*, 1992]. However, a re-interpretation of the ESP 5 (Figure 3e), using seismic profiles to correlate the deeper refraction arrivals observed on this ESP (Figure 3d), concluded that a 4.7–4.8 km/s layer at 8.4 s TWT depth (9.4 km depth) may have a sedimentary origin because of its layered facies [*Le Meur*, 1997]. Analysis of the Archimede (Figure 3a) and PrisMed01 profiles (Figure 4) confirms this layered facies and the 4.7–5 km/s velocity layer (Figure 3b), called ambiguous unit, may have a sedimentary origin. The thickness of the resulting oceanic crust recognized beneath the IAP is then 7.2 km thick (Figure 3f) [*Le Meur*, 1997], more consistent with the thickness of typical oceanic crust [*White et al.*, 1992].

3.2. Deformation of the Sediments Beneath the Ionian Abyssal Plain

[20] Beneath the Ionian Abyssal Plain, the entire sedimentary sequence is deformed. However, this deformation is the consequence of two decoupled tectonic processes. On the one hand, thin skinned SE vergent thrust faulting affects the Messinian Mobile and Upper Units and the Plio-Quaternary deposits, which are accreted to the Calabrian prism. On the other hand, thick skinned (crustal scale) NW vergent reverse faulting affected the pre-evaporitic deposits.

[21] Northwest of the Ionian Abyssal Plain, we observe closely spaced SE vergent thrusts (Figure 4a, s.p. 4000 to 5300). These lead to anticlinal folding and thrusting of the Messinian Mobile and Upper Units and of the Plio-Quaternary sediments (Figure 6) [*Chamot-Rooke et al.*, 2005; *Minelli and Faccenna*, 2010]. The base of the Messinian Mobile Unit was interpreted as the basal decollement in the frontal part of the post-Messinian Calabrian wedge, thus the post-evaporitic (Messinian Mobile Unit) sediments are accreted to the Calabrian prism above the B-reflector (Figure 4a) [*Chamot-Rooke et al.*, 2005; *Minelli and Faccenna*, 2010]. Successive imbricate thrusting and some back thrusting within the Calabrian prism allow a doubling of the thickness of this sequence within 30 km of the deformation front (Figure 4a).

[22] Beneath the Ionian Abyssal Plain, large-scale anticlines affect the entire sedimentary cover from the oceanic basement to the B-reflector, at the base of the Messinian Mobile Unit (Figures 4–6). The geometry of these anticlines with short and steep forelimbs (Figures 4 and 5) and a significant vertical offset of the top of oceanic basement (e.g., fault F5 (Figure 4, s.p. 5750, and Figure 5, s.p. 3060)) allows us to define a set of reverse crustal faults. The activity of these 60 to 65° dipping faults led to the development of basins over 1 km in thickness (Figures 4c and 5c, the dark red reflectors). They are filled with the Tortonian syntectonic unit, which exhibits an onlapping growth strata facies (Figures 4 and 5). These Tortonian sediments were deposited synchronously to the fault activity. The seismic velocities for these sediments (2.6 to 2.8 km/s) are particularly low for strata at 6 km depth, overlain by more than 1.5 km thick Messinian and Plio-Quaternary layer (Figures 4b and 5b). This low velocity could be caused by high porosity and fluid overpressure in the sediments, which may reduce the velocities of the sediments below the undisturbed impermeable evaporitic layer. This layer (Messinian Mobile Unit) acts like a caprock, which may lead to stagnation and subsequent overpressure in the sediment below. We note that the internal velocities obtained during the PSDM (Figures 4b and 5b) are slightly lower than the velocities obtained with the ESP 5 results (Figures 3b and 3d). This may be explained by anisotropy of sedimentary units in response to the near-vertical propagation path in reflection seismic compared to the near horizontal propagation path in refraction seismic, with approximately 10% higher horizontal velocities [*Bartolome et al.*, 2005]. On the depth seismic lines, the base of Messinian Mobile Unit is slightly folded on top of the main NW vergent faults (F4, F5, F6 and F7, Figures 4 and 5). This implies that these crustal faults may have been active from the Tortonian, characterized by syntectonic sedimentation to the early Messinian times.

[23] The large vertical offsets (reaching 1.5 km) of the top of the basement along major faults allow us to establish a line to line correlation through the Ionian Abyssal Plain (Figure 6). 100 km long SW-NE trending faults are interpreted as crustal reverse faults, mostly NW vergent and with a typical spacing of 10 to 20 km (Figures 4–6). A series of NE-SW trending morphologic highs (VHStr., VSH 2, NaStr., VaStr., Figure 2) and their control on the depocenters of evaporites were pointed out by earlier seismic studies [*Hieke et al.*, 2003, 2006]. The VHS Structure, the northward SW-NE trending prolongation of the VHS 2, was interpreted as an extensional structure (a horst), formed by extension of continental crust [*Hieke et al.*, 2003, 2006]. On the profiles, no Messinian sediment is observed over the VHS 2, and a 880 m thick small evaporitic basin develops between the Nathalie Structure and the VHS 2 (Figures 4 and 5). We confirm that the VHS 2 corresponds to a structural high formed mainly in the pre-Messinian times [*Hieke et al.*, 2003]. Our seismic data clearly show that the VHS 2 and the Nathalie Structure are tectonic pop-up structures, formed in response to the activity of the NW and SE associated vergent faults F1/F2 and F3/F4, respectively (Figures 4–6). In this compressive framework, the Valvidia Structure corresponds to an anticlinal fold, formed in response to the activity of the major 65° dipping and NW vergent fault F5 (Figures 4 and 5). After examination of

Figure 5. Zoom on the pre-stack depth migrated Archimede 19 profile (no vertical exaggeration). (a) On the line drawing, see (1) the thin skinned SE vergent thrust faulting caused by the accretion of post-evaporitic (Messinian Mobile Unit) deposits, forming the Calabrian prism (s.p. 2220 (deformation front) to 1500), and (2) the thick skinned (crustal scale) NW vergent reverse faulting (s.p. 3750 to 1900). (b) Portion of the profile Archimede 19 line in depth (with the internal velocity model obtained during depth migration). (c) Line drawing of the extract showing the geometry of reverse faults, with dips ranging from 60 to 65°. Note the presence of well-developed Tortonian syntectonic basins (dark red reflectors, s.p. 2750 to 2900 and s.p. 2800 to 3100) and their link with the morphologic highs (Nathalie and Valvidia Structures and VHS 2).

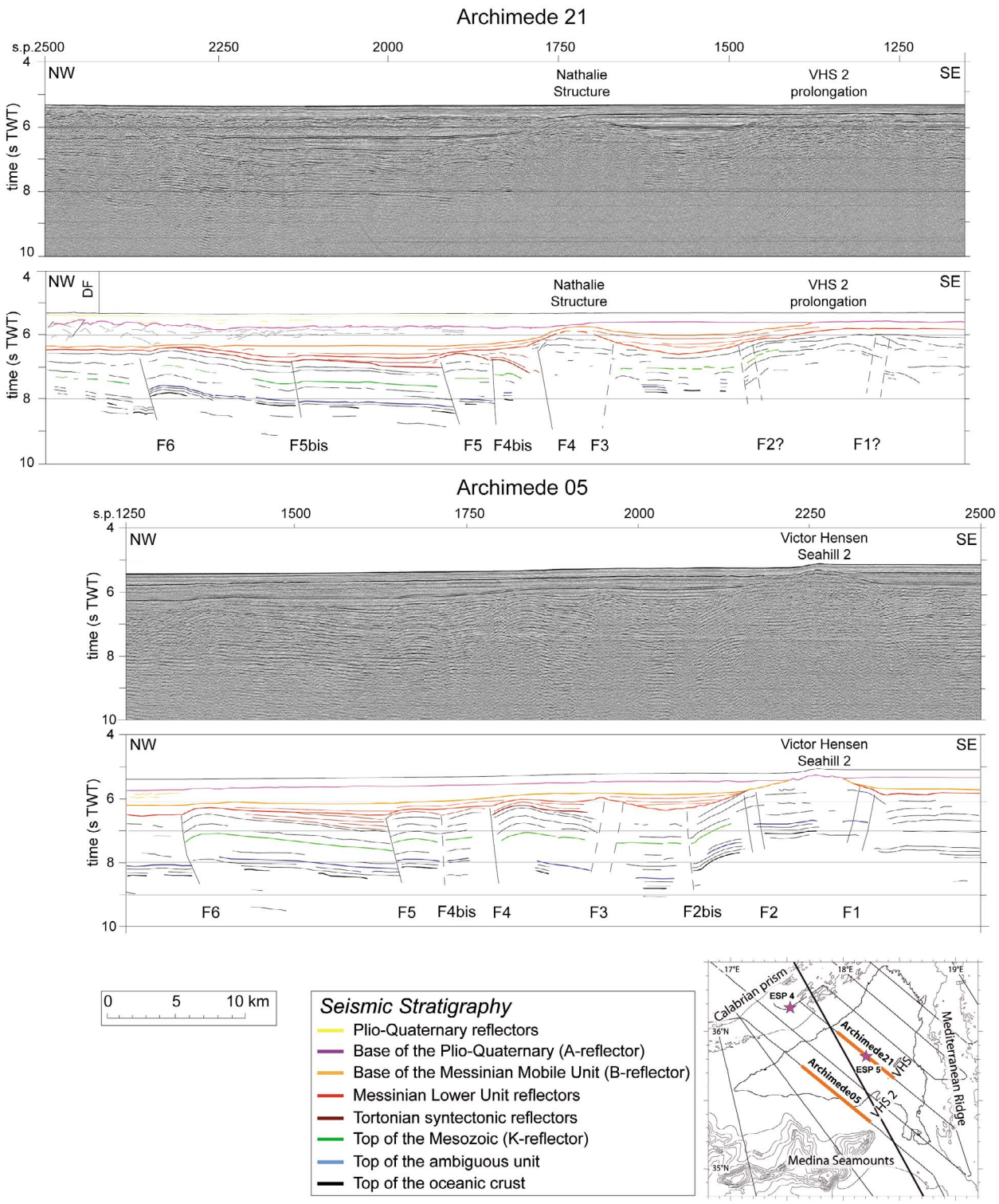

Figure 6. Portions of the Archimede 05 and 21 profiles (time migrated) showing the morphologic highs and their link to the mostly NW vergent reverse faults (vertical exaggeration of 6, see position in Figure 2). Note the homogenous geometry of the fault pattern through the IAP, which allows the line to line correlation.

the seismic lines published on the VHS [see *Hieke et al.*, 2003, Figure 4e; *Hieke et al.*, 2006], we interpret it as a purely diapiric salt structure. Using trigonometry, the dip angle of the faults and the offset of the top of oceanic crust, we estimate the shortening accommodated beneath the Ionian Abyssal Plain. We show that on the PrisMed01 line, 4.1 km of shortening is accommodated over a 82 km long section, corresponding to a bulk shortening of 5%. On the

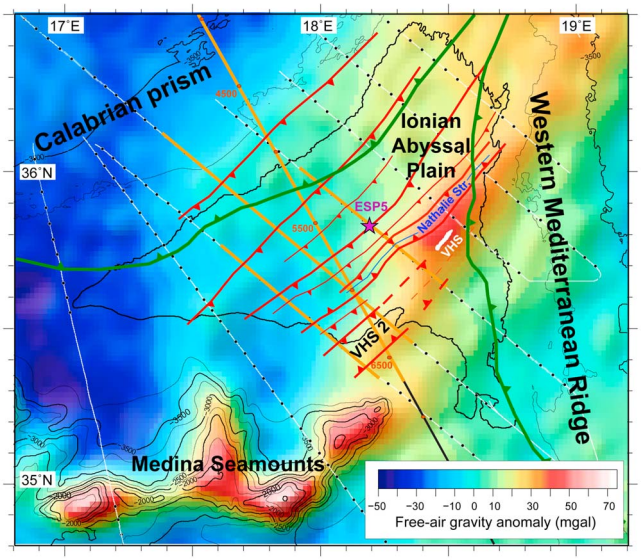

Figure 7. Tectonic map of the Ionian Abyssal Plain showing the N55°E striking deep faults primarily NW vergent (red lines) beneath the Ionian Abyssal Plain. The positions of the deformation fronts of the Calabrian prism and Western Mediterranean Ridge are shown in green (interpreted from the seismic lines). The free-air gravity anomaly is shown using the rainbow color scale (Version 16.1, see *Sandwell and Smith* [2009] for references) and the bathymetric contours (each 500 m) in black, with the crustal highs (GEBCO 1 min and Medimap Group Bathymetry compilation [*Loubrieu et al.*, 2007]). Thick orange lines indicate the profiles shown in the paper.

line Archimede 19, we find 3 km of shortening accommodated over a 85 km long section, equivalent to a bulk shortening of 3.5%.

[24] The free-air gravity anomaly also provides constraints on the deep crustal structure beneath the Ionian Abyssal Plain (Figure 7), where more than 5 km of sediments are deposited (Figure 4) (Version 16.1 of *Sandwell and Smith* [2009, and references therein]). The free-air gravity anomaly clearly reveals SW-NE trending features in the southern Ionian Abyssal Plain, characterized by positive gravity anomalies (Figure 7). The Medina Seamounts show the highest value (>50 mgal) and a clear prolongation of the Medina Seamounts is expressed in the gravity anomaly through the VHS 2 to the Nathalie Structure (Figure 7). These high values suggest the presence of excess mass at depth directly beneath the morphologic highs and subbottom structures. The free-air gravity anomaly map confirms the basement involvement of the NE-SW trending structures described above. We suggest that the mass excess may also be related to a local tectonic uplift of the Moho.

[25] To conclude, two types of compressive deformation are clearly expressed beneath the Ionian Abyssal Plain and are decoupled: recent accretion above the B-reflector forming the Calabrian prism NW of the IAP, and an older episode of large-scale crustal deformation, expressed as SW-NE trending reverse faults, associated with morphologic highs. Using the constraints offered by the seismic stratigraphy and the paleogeographic reconstructions of the Ionian basin, we will now discuss the origin of these reverse faults and the timing of their activity.

4. Discussion

4.1. Origin of the Deep Reverse Faults Beneath the Ionian Abyssal Plain

[26] A major question raised by this study: What is the origin of the faults, which have been reactivated beneath the Ionian Abyssal Plain? Within the framework of existing paleogeographic models for the evolution of the Mediterranean basins, different hypotheses can be proposed: (a) flexural bending faults, (b) transform faults or (c) normal faults related to seafloor spreading of the Ionian basin.

[27] (a) Outboard of subduction zones, a flexural bulge develops on the subducting plate, which can produce extensional bending faults. Such normal faults typically form approximately 50 to 100 km away from the trench. We show that the reactivation of the 55°N trending faults occurred in the Tortonian times, with the development of syntectonic basins (see section 3.2). During the Tortonian, the front of the Ionian subduction was located several hundred km further to the NW (Figure 7) [*Faccenna et al.*, 2001]. Any normal bending faults, which may have formed on the downgoing plate during the Tortonian would have been already consumed by the subduction processes. Thus, this hypothesis can be discarded.

[28] (b) In Central Mediterranean, the Malta escarpment (Figure 1) was for a long time considered as part of a passive margin separating the continental domain of Sicily and of the Pelagian Sea from the deep Ionian oceanic basin [*Scandone et al.*, 1981; *Jongsma et al.*, 1985, 1987; *Groupe Escarmed et al.*, 1988; *Catalano et al.*, 2001; *Argnani and Bonazzi*, 2005]. Some researchers interpreted the Apulian escarpment (Figure 1) to be the conjugate of the Malta escarpment and thus that the Ionian Sea had opened in a NE-SW direction [*Catalano et al.*, 2001; *Chamot-Rooke et al.*, 2005]. According to this framework, the 55°N trending set of faults we have identified would be almost parallel to the opening direction and could correspond to a pattern of transform faults. We show that the pattern of faults beneath the IAP dips at 60–65° and was reactivated. Oceanic transforms faults are typically sub-vertical faults [*De Long et al.*, 1977], and thus would be very difficult to reactivate in a perpendicular compressive stress field. So both the geometry of the fault pattern beneath the IAP and its reactivation are in disagreement with the hypothesis of a transform fault origin.

[29] (c) Very recently, it was proposed that the Ionian basin opened NW-SE following a late Triassic-early Jurassic rifting [*Frizon de Lamotte et al.*, 2011; *Raulin et al.*, 2011]. The SW-NE orientation of the faults beneath the IAP suggests that they could have initially formed as normal faults during the spreading of the Ionian basin. After comparison of this fault pattern with the Atlantic and Indian oceanic fabrics, the oceanic nature of the Ionian basin [*de Voogd et al.*, 1992] together with fault dip (60–65°) are clearly consistent with a normal fault origin [*Sykes*, 1967; *Choukroune et al.*, 1984; *Bull and Scrutton*, 1992]. The fault spacing (20 km) is also in good agreement with the observed oceanic

fabric morphology observed in the Canary basin [*Ranero and Banda*, 1997] and in the West Philippine basin, adjacent to an abandoned spreading axis [*Deschamps et al.*, 2002]. We propose that the fault pattern beneath the IAP was initially a set the SW-NE trending oceanic normal faults, formed during the NW-SE opening of the Ionian basin [*Frizon de Lamotte et al.*, 2011; *Raulin et al.*, 2011].

[30] According to this framework, the Malta escarpment would be part of a continental transform margin separating the continental domain of Sicily and of the Pelagian Sea from the deep Ionian oceanic basin [*Frizon de Lamotte et al.*, 2011]. The abrupt crustal thinning across the escarpment (from 30 to 10 km) [*Makris et al.*, 1986] and the presence of only few titled blocks [*Nicolich et al.*, 2000] along this escarpment is consistent with a transform fault origin [*De Long et al.*, 1977; *Mascle and Basile*, 1988]. The ocean/continent transition is considered to occur 50 km eastward of the Malta escarpment [*Chamot-Rooke et al.*, 2005], this suggests that the crustal thinning toward the Ionian basin occurs across a very narrow region. This is also in good agreement previous observations of continental transform margins [*Benkhelil et al.*, 1995; *Mascle and Basile*, 1988; *Edwards et al.*, 1997; *Lamarche et al.*, 1997; *Sage et al.*, 1997; *Sallarès et al.*, 2011]. The NNW-SSE trending Malta escarpment may be the expression of an initial rifting setting as a transform margin during the Triassic-Jurassic rifting of the Ionian basin (Figure 8). The increase of the heat flow measurements at the northern edge of the Medina Seamounts, just southeast of the Malta escarpment, also suggests that a transition in the nature of the basement occurs [*Pasquale et al.*, 2005, Figure 1]. The seafloor morphology of the Medina Seamounts, characterized by "en echelon" features, with a stair-case pattern alternating between NNW-SSE trending elements and WSW-ENE trending segments (Figure 2) is also consistent with a Gondwana rifted margin (Figure 7).

[31] Following all these points, we conclude that the SW-NE trending faults beneath the IAP are remnant crustal faults of the NW-SE Ionian oceanic spreading, that developed in a continental transform margin framework along the Malta escarpment.

4.2. Intraplate Deformation Beneath the Ionian Abyssal Plain

[32] We show that the set of deep reverse faults present beneath the IAP is a remnant of the seafloor spreading fabric formed during the Jurassic-Cretaceous NW-SE opening of the Ionian basin (Figure 8) [*Frizon de Lamotte et al.*, 2011]. But we also clearly show that on the seismic lines, the activity of these crustal scale features led to the formation of anticlines and Tortonian syntectonic basins. Below we will discuss the possibility of inverting an oceanic domain under compressive stress and the timing of the inversion.

[33] Based on the plate tectonic model, it was assumed that the rigid oceanic lithosphere, with respect to continental lithosphere, would remain relatively undeformed during its growth and destruction. However, during tectonic inversion normal and transform faults originally formed at spreading centers may be reactivated in areas of diffuse intraplate deformation [*Delescluse et al.*, 2008]. This reverse reactivation of normal faults during basin inversion has been studied by analog modeling studies [*Koopman et al.*, 1987; *Mandal and Chattopadhyay*, 1995; *Konstantinovskaya et al.*, 2007]. These studies conclude that the inversion of normal faults is feasible and depends on their initial geometry and orientation with respect to the direction of compression [*Mandal and Chattopadhyay*, 1995; *Konstantinovskaya et al.*, 2007]. Theoretical analyses show that the fluid pressure may greatly enhance reactivation by lowering the resistance along the fault zone [*Etheridge*, 1986]. We consider that the high-amplitude of the reflectors beneath the IAP and the low internal velocity are also a sign of the presence of fluids, which may have played a role during the reactivation of the original oceanic fabric (see section 3.2).

[34] The Central Indian Ocean basin is the best documented area, where intraplate deformation occurs under compressive stress [*Bull and Scrutton*, 1992; *Delescluse et al.*, 2008]. Multichannel seismic images of the Central Indian Ocean basin allow the identification of reactivated paleo-normal faults, with a characteristic fault-block width of 5 to 20 km [*Bull and Scrutton*, 1992]. A set of north-dipping reverse basement faults is observed with associated hanging wall anticlines. Their dips range from 30 to 40° in the basement with a rapid increase to dips >65° in the sedimentary cover. This fault pattern is interpreted to be the result of reactivation of pre-existing normal faults originally formed at the spreading center [*Bull and Scrutton*, 1992]. In the Ionian basin, the fault spacing (10 to 20 km) together with the steep fault dips of the fault (60 to 65°) allow us to propose a similar evolution: an Ionian seafloor spreading fabric, acquired during the Jurassic-Cretaceous opening of the basin and reactivated later during the Tortonian-early Messinian times (Figure 8). Recent numerical modeling shows that the entire fault network formed at the Central Indian Ocean ridge axis was initially reactivated, but that only a small fraction of these faults remained active through time and accumulated significant displacements [*Delescluse et al.*, 2008]. These long-lived major, active faults bound blocks, which are modeled at a spacing of 20 to 30 km [*Delescluse et al.*, 2008], in good agreement with seismic lines [*Bull and Scrutton*, 1992]. The 20 km spacing faults pattern of the IAP fits well with modeling results obtained for the Central Indian Ocean [*Delescluse et al.*, 2008]. Beneath the IAP, our data set suggests that the overall set of faults may have been active during the early stage of the reactivation during the Tortonian (Figures 4 and 5). Later, it seems that a selective abandonment of the faults called "F…bis" occurs in early Messinian times during the deposit of Messinian Lower Unit (Figure 7). In fact, on top of these faults, the base of Messinian Mobile Unit is not folded. Only some major faults (faults "F…") show significant evidence of long-lived activity. The compression along the major faults (referred as F4, F5 and F6) led to the development of 1 km thick Tortonian syntectonic basins, and folding of the base of the Messinian Mobile Unit (Figures 4 and 5). The fault activity seems to stop or slow down after the early Messinian, since no deformation is observed in late Messinian sediments.

4.3. Causes of Intraplate Deformation of the Ionian Basin

[35] In this section, we will discuss the possible causes of this intraplate deformation and its significance within the framework of the evolution of the Central Mediterranean.

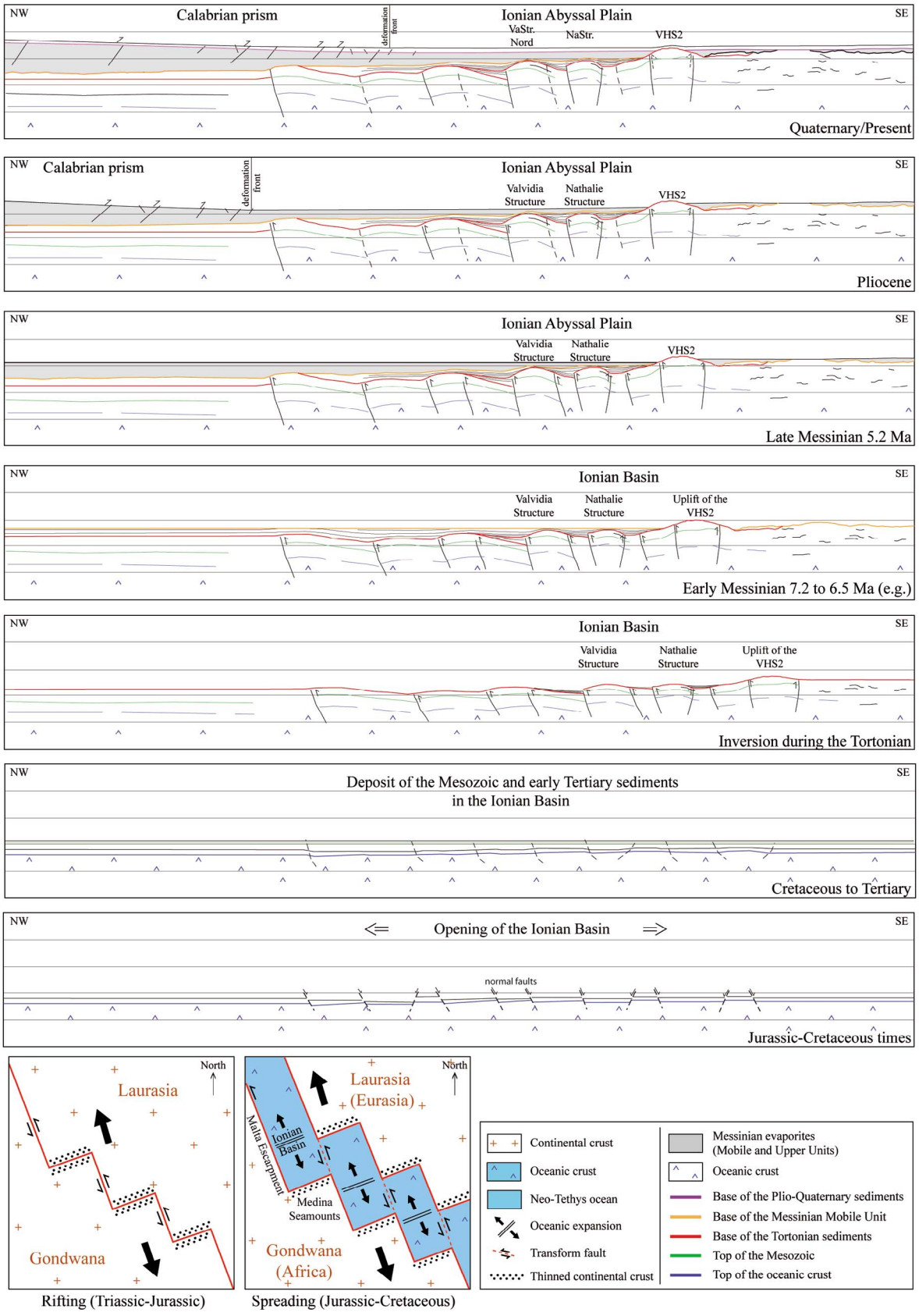

Figure 8. (bottom) Tectonic sketches of the NW-SE rifting of the Ionian basin during the Triassic-Jurassic times and the subsequent spreading and (top) seven schematic SE-NW cross-sections showing the evolution the Ionian basin, north of the Gondwana (Africa) margin from the Jurassic-Cretaceous to the Present.

Based on the evolution of the regions adjacent to the Ionian sea, different causes can be invoked to explain the compressive reactivation of oceanic fabric of the Ionian basin: (a) the Alpine collision, (b) the Southeastward drift of Calabria, (c) the motion of an independent Ionian microplate.

[36] (a) On the basis of seismic correlations from the Gulf of Sirte to the Ionian Abyssal Plain, the refracted arrivals at 6.7 s TWT depth were proposed to correspond to the top of the Mesozoic (Figure 3b) [*de Voogd et al.*, 1992]. These authors outlined that these correlations were made with "less certainty" for the data located beneath the Ionian Abyssal Plain [*de Voogd et al.*, 1992; *Sioni*, 1996]. This led other authors to propose the reflector at 6.6 sTWT to be the top of the Mesozoic sequence, and to imply that the syntectonic sediments have to be older than the Tortonian [*Sioni*, 1996; *Minelli and Faccenna*, 2010]. Then, the tectonic reactivation was proposed to be caused by a narrowing of this Mediterranean domain in response to the Alpine collision in the pre-Miocene times [*Sioni*, 1996]. However, we follow the first seismic interpretation proposed for the top of the Mesozoic (section 3.1), identified at 7.25 s TWT depth [*Finetti and Morelli*, 1972]. So we discard the Alpine collision hypothesis for the observed deformation beneath the Ionian Abyssal Plain.

[37] (b) Other seismic facies correlations, established East of the Malta escarpment [*Cernobori et al.*, 1996; *Chamot-Rooke et al.*, 2005] led to an interpretation of the Messinian Lower Unit together with the Tortonian syntectonic unit of this study (see section 3.1) as a single syntectonic Tortonian-Serravallian unit [*Chamot-Rooke et al.*, 2005]. After careful interpretations, we propose that the unit below the Messinian Mobile Unit also corresponds to Messinian sediments (Figure 3a) [*Lofi et al.*, 2011a]; and that only the sediments deposited in sub-basins are syntectonic. The consequence is the same age of initial reactivation (Tortonian) (Figure 8), but a reduced sedimentary record of the inversion of the Ionian basin. We also show that the base of the Messinian Mobile Unit is folded. Therefore, the tectonic inversion has continued at least until the early Messinian times (Figure 8). The timing of this inversion is consistent with the geodynamic evolution of the Western Mediterranean domain.

[38] After the cessation of the counterclockwise rotation of the Corsica-Sardinia block around 15 Ma, a period of tectonic reorganization occurred [*Malinverno and Ryan*, 1986; *Faccenna et al.*, 2004]. Soon afterwards more rapid NW subduction and related to the SE directed roll-back of the Ionian slab occurred together with the opening of the Tyrrhenian Sea in the Miocene [*Malinverno and Ryan*, 1986; *Gueguen et al.*, 1998; *Jolivet and Faccenna*, 2000; *Faccenna et al.*, 2001; *Chiarabba et al.*, 2008]. We propose that the Tortonian-early Messinian inversion occurred during this reorganization phase (Figure 8). Then the accommodation of both the compression due to the slab roll-back of the Calabrian block and the subduction of the Ionian lithosphere was partly transferred to the Ionian basin, reactivating the inherited oceanic fabric.

[39] (c) Based on GPS results, a current intraplate deformation of an Ionian microplate cannot be excluded, in particular North of the Ionian Abyssal Plain [*Anzidei et al.*, 1996]. Based on the lack of seismicity and the absence of deformation in the Plio-Quaternary deposits along the Apulian escarpment, newly published GPS data support the interpretation that Apulia together with the Ionian Sea form a single microplate [*D'Agostino et al.*, 2008, 2011]. This Ionian-Apulian microplate is rotating relative to Nubia, around the GPS-derived Eulerian pole located in the Gulf of Sirte (Figure 1) [*D'Agostino et al.*, 2008]. This rotation accommodates a fraction of the convergence between Africa and Eurasia and may still drive limited intraplate compression beneath the Ionian Abyssal Plain [*Jongsma et al.*, 1985, 1987]. We are not able to discard the hypothesis of persistent activity of this network of faults beneath the IAP on the basis of multichannel seismic data. Further GPS measurement may offer a chance to better discuss the present-day activity of these faults.

[40] To conclude, we wish to emphasize that the proposed timing of the inversion of the Ionian basin is controlled by the answer to the crucial question: "What is the age of the syntectonic unit"?, without direct evidence from drill hole. We argue that the syntectonic units are Tortonian sediments, and suggest the inversion of the Ionian basin may be linked to a plate reorganization at that times. On the basis of the recent GPS, ongoing but less vigorous compression cannot be ruled out.

5. Conclusions

[41] In this study, we analyzed a set multichannel seismic profiles (Archimede and PrisMed cruises). These seismic images reveal a set of well-developed N55°E striking large-scale, reverse faults primarily NW vergent and linked to hanging wall anticlines beneath the Ionian Abyssal Plain. A comparison with the best-documented oceanic intraplate deformed area, the Central Indian Ocean leads us to interpret that this set of 10 to 20 km spaced crustal reverse faults as reactivated normal faults. In agreement with very recent paleogeographic studies, we propose that the fault pattern of the Ionian basin formed as a seafloor spreading fabric acquired after the late Triassic-early Jurassic rifting setting as a transform margin along the Malta escarpment. This study also leads to the interpretation of a new stratigraphic succession over the oceanic crust beneath the Ionian Abyssal Plain. In the Central Mediterranean domain, the identification of a Messinian Lower Unit, previously identified as Tortonian in age, leads to a revision in the timing of the inversion of the Ionian basin. We propose that these 60 to 65° dipping inherited normal faults were reactivated as reverse faults during the Tortonian, forming syntectonic basins. The folding of the base Messinian Mobile Unit suggests continued but reduced activity of some major faults until the early Messinian. Our results indicate a total shortening of 3–4 km distributed over a NW-SE 80 km wide and a NE-SW 200 km long zone with a bulk shortening of 3.5–5%, values characteristic for diffuse intraplate deformation. This deformation of the Ionian domain is interpreted to be related to a plate tectonic reorganization prior to the rapid southeastward drift of Calabria, associated with the main phase of back-arc opening of the Tyrrhenian domain. Based on recent GPS studies, the independent rotation of a Ionian-Apulian microplate in the Central Mediterranean may cause residual minor deformation beneath the IAP.

[42] **Acknowledgments.** The authors thank Jacques Déverchère, Johanna Lofi and Pierre Strzerzynski for constructive comments of early versions of this paper and for enlightening discussions about the Messinian in the Mediterranean domain. Marcia Maia is thanked for helpful comments on the gravity anomalies. We thank Jean Mascle for the seismic data of the PrisMed01 line and the opportunity to process this long transect. We gratefully acknowledge Marc Schaming and Laure Schenini their help for reading in reading these data with the GeoVecteur Software. The maps were drafted using the Generic Mapping Tools (GMT) software [*Wessel and Smith*, 1991].

References

Anzidei, M., P. Baldi, G. Casula, M. Crespi, and F. Riguzzi (1996), Repeated GPS surveys across the Ionian Sea: Evidence of crustal deformations, *Geophys. J. Int.*, *127*, 257–267, doi:10.1111/j.1365-246X.1996.tb04718.x.

Argnani, A., and C. Bonazzi (2005), Malta Escarpment fault zone offshore eastern Sicily: Plio-Quaternary tectonic evolution based on new multichannel seismic data, *Tectonics*, *24*, TC4009, doi:10.1029/2004TC001656.

Avedik, F., A. Hirn, R. Nicolich, J. L. Olivet, and M. Sachpazi (1996), "Single-bubble" marine source offers new perspectives for lithospheric exploration, *Tectonophysics*, *267*, 57–71, doi:10.1016/S0040-1951(96)00112-6.

Bartolome, R., I. Contrucci, H. Nouze, E. Thiebot, and F. Klingelhoefer (2005), Using the OBS wide-angle reflection/refraction velocities to perform a pre-stack depth migration image of the "single bubble" multichannel seismic: Example of the Moroccan margin, *J. Appl. Geophys.*, *57*, 107–118, doi:10.1016/j.jappgeo.2004.10.004.

Benkhelil, J., J. Mascle, and P. Tricart (1995), The Guinea continental margin: An example of a structurally complex transform margin, *Tectonophysics*, *248*, 117–137, doi:10.1016/0040-1951(94)00246-6.

Bull, J. M., and R. A. Scrutton (1992), Seismic reflection images of intraplate deformation, central Indian Ocean, and their tectonic significance, *J. Geol. Soc.*, *149*, 955–966, doi:10.1144/gsjgs.149.6.0955.

Catalano, S., C. Doglioni, and S. Merlini (2001), On the Mesozoic Ionian Basin, *Geophys. J. Int.*, *144*, 49–64, doi:10.1046/j.0956-540X.2000.01287.x.

Cernobori, L., et al. (1996), Crustal image of the Ionian basin and its Calabrian margins, *Tectonophysics*, *264*, 175–189, doi:10.1016/S0040-1951(96)00125-4.

Chamot-Rooke, N., C. Rangin, X. Le Pichon, and Dotmed Working Group (2005), DOTMED—Deep Offshore Tectonics of the Mediterranean: A synthesis of deep marine data in eastern Mediterranean, *Mem. Soc. Geol. Fr.*, *177*, 64 pp., 69 maps with CD-ROM.

Chiarabba, C., L. Jovane, and R. DiStefano (2005), A new view of Italian seismicity using 20 years of instrumental recording, *Tectonophysics*, *395*, 251–268, doi:10.1016/j.tecto.2004.09.013.

Chiarabba, C., P. De Gori, and F. Speranza (2008), The southern Tyrrhenian subduction zone: Deep geometry, magmatism and Plio-Pleistocene evolution, *Earth Planet. Sci. Lett.*, *268*, 408–423, doi:10.1016/j.epsl.2008.01.036.

Choukroune, P., J. Francheteau, and R. Hekinian (1984), Tectonics of the East Pacific Rise near 12°50′N: A submersible study, *Earth Planet. Sci. Lett.*, *68*, 115–127, doi:10.1016/0012-821X(84)90144-4.

Cita, M. B., and B. Rimoldi (1997), Geological and geophysical evidence for a Holocene tsunami deposit in the eastern Mediterranean deep-sea record, *J. Geodyn.*, *24*, 293–304, doi:10.1016/S0264-3707(96)00030-0.

D'Agostino, N., A. Avallone, D. Cheloni, E. D'Anastasio, S. Mantenuto, and G. Selvaggi (2008), Active tectonics of the Adriatic region from GPS and earthquake slip vectors, *J. Geophys. Res.*, *113*, B12413, doi:10.1029/2008JB005860.

D'Agostino, N., E. D'Anastasio, A. Gervasi, I. Guerra, M. R. Nedimović, L. Seeber, and M. Steckler (2011), Forearc extension and slow rollback of the Calabrian Arc from GPS measurements, *Geophys. Res. Lett.*, *38*, L17304, doi:10.1029/2011GL048270.

Delescluse, M., L. G. J. Montési, and N. Chamot-Rooke (2008), Fault reactivation and selective abandonment in the oceanic lithosphere, *Geophys. Res. Lett.*, *35*, L16312, doi:10.1029/2008GL035066.

De Long, S. E., J. F. Dewey, and P. J. Fox (1977), Displacement history of oceanic fracture zones, *Geology*, *5*, 199–202, doi:10.1130/0091-7613(1977)5<199:DHOOFZ>2.0.CO;2.

DeMets, C., G. Gordon, D. F. Argus, and S. Stein (1994), Effects of recent revisions to the geomagnetic reversal time scale on estimates of current plate motions, *Geophys. Res. Lett.*, *21*, 2191–2194, doi:10.1029/94GL02118.

Dercourt, J., et al. (1986), Geological evolution of the Tethys belt from the Atlantic to the Pamirs since the Lias, *Tectonophysics*, *123*, 241–315, doi:10.1016/0040-1951(86)90199-X.

Deschamps, A., K. Okino, and K. Fujioka (2002), Late amagmatic extension along the central and eastern segments of the West Philippine Basin fossil spreading axis, *Earth Planet. Sci. Lett.*, *203*, 277–293.

de Voogd, B., et al. (1992), Two-ship deep seismic soundings in the basins of the eastern Mediterranean Sea (Pasiphae cruise), *Geophys. J. Int.*, *109*, 536–552, doi:10.1111/j.1365-246X.1992.tb00116.x.

Di Bucci, D., P. Burrato, P. Vannoli, and G. Valensise (2010), Tectonic evidence for the ongoing Africa-Eurasia convergence in central Mediterranean foreland areas: A journey among long-lived shear zones, large earthquakes, and elusive fault motions, *J. Geophys. Res.*, *115*, B12404, doi:10.1029/2009JB006480.

Edwards, R. A., R. B. Whitmarsh, and R. A. Scrutton (1997), Synthesis of the crustal structure of the transform continental margin off Ghana, northern Gulf of Guinea, *Geo Mar. Lett.*, *17*, 12–20, doi:10.1007/PL00007202.

Etheridge, M. A. (1986), On the reactivation of extensional fault system, *Philos. Trans. R. Soc. London, Ser. A*, *317*, 179–194, doi:10.1098/rsta.1986.0031.

Faccenna, C., F. Funiciello, D. Giardini, and F. P. Lucente (2001), Episodic back-arc extension during restricted mantle convection in the central Mediterranean, *Earth Planet. Sci. Lett.*, *187*, 105–116, doi:10.1016/S0012-821X(01)00280-1.

Faccenna, C., C. Piromallo, A. Crespo-Blanc, L. Jolivet, and F. Rossetti (2004), Lateral slab deformation and the origin of the western Mediterranean arcs, *Tectonics*, *23*, TC1012, doi:10.1029/2002TC001488.

Finetti, I. (1982), Structure, stratigraphy and evolution of Central Mediterranean, *Bol. Geofis. Teor. Appl.*, *XXIV*(96), 247–312.

Finetti, I., and A. Morelli (1972), Wide scale digital seismic exploration of the Mediterranean Sea, *Bol. Geofis. Teor. Appl.*, *XIV*(56), 291–342.

Frizon de Lamotte, D., C. Raulin, N. Mouchot, J.-C. Wrobel-Daveau, C. Blanpied, and J.-C. Ringenbach (2011), The southernmost margin of the Tethys realm during the Mesozoic and Cenozoic: Initial geometry and timing of the inversion processes, *Tectonics*, *30*, TC3002, doi:10.1029/2010TC002691.

Garfunkel, Z. (1998), Constrains on the origin and history of the eastern Mediterranean basin, *Tectonophysics*, *298*, 5–35, doi:10.1016/S0040-1951(98)00176-0.

Golonka, J. (2004), Plate tectonic evolution of the southern margin of Eurasia in the Mesozoic and Cenozoic, *Tectonophysics*, *381*, 235–273, doi:10.1016/j.tecto.2002.06.004.

Groupe Escarmed, S. Charier, B. Biju-Duval, Y. Morel, and S. Rossi (1988), L'escarpement Apulien et le promontoire de Céphalonie: Marge septentrionale du bassin Ionien (synthèse des données des campagnes à la mer Escarmed), *Oil Gas Sci. Technol.*, *43*, 485–515.

Gueguen, E., C. Doglioni, and M. Fernandez (1998), On the post-25 Ma geodynamic evolution of the western Mediterranean, *Tectonophysics*, *298*, 259–269, doi:10.1016/S0040-1951(98)00189-9.

Guiraud, R., W. Bosworth, J. Thierry, and A. Delplanque (2005), Phanerozoic geological evolution of northern and central Africa: An overview, *J. Afr. Earth Sci.*, *43*, 83–143, doi:10.1016/j.jafrearsci.2005.07.017.

Handy, M. R., S. M. Schmid, R. Bousquet, E. Kissling, and D. Bernouilli (2010), Reconciling plate-tectonic reconstructions of Alpine Tethys with the geological-geophysical record of spreading and subduction in the Alps, *Earth Sci. Rev.*, *102*, 121–158, doi:10.1016/j.earscirev.2010.06.002.

Hieke, W. (1978), The "Victor Hensen Seahill"; part of a tectonic structure in the central Ionian sea, *Mar. Geol.*, *26*, M1–M5, doi:10.1016/0025-3227(78)90051-8.

Hieke, W. (1984), A thick Holocene homogenite from the Ionian Abyssal Plain (Eastern Mediterranean), *Mar. Geol.*, *55*, 63–78, doi:10.1016/0025-3227(84)90133-6.

Hieke, W., and A. Wanninger (1985), The Victor Hensen Seahill (central Ionian Sea)—Morphology and structural aspects, *Mar. Geol.*, *64*, 343–350, doi:10.1016/0025-3227(85)90112-4.

Hieke, W., and F. Werner (2000), The Augias megaturbidites in the central Ionian Sea (central Mediterranean) and its relation to the Holocene Santorini event, *Sediment. Geol.*, *135*, 205–218, doi:10.1016/S0037-0738(00)00072-5.

Hieke, W., H. B. Hirschleber, and G. A. Dehghani (2003), The Ionian Abyssal Plain (central Mediterranean Sea): Morphology, subbottom structures and geodynamic history–an inventory, *Mar. Geophys. Res.*, *24*, 279–310, doi:10.1007/s11001-004-2173-z.

Hieke, W., M. B. Cita, F. Forcella, and C. Müller (2006), Geology of the Victor Hensen Seahill (Ionian Sea, eastern Mediterranean): Insights from the study of cored sediment sequences, *Boll. Soc. Geol. Ital.*, *125*, 245–257.

Hollenstein, C., H.-G. Kahle, A. Geiger, S. Jenny, S. Goes, and D. Giardini (2003), New GPS constraints on the Africa-Eurasia plate boundary zone in southern Italy, *Geophys. Res. Lett.*, *30*(18), 1935, doi:10.1029/2003GL017554.

Hsü, K. J., L. Montard, R. B. Garrison, F. H. Fabricius, R. B. Kidd, C. Müller, M. B. Cita, G. Bizon, R. C. Wright, and A. J. Erickson (1978), Site 374: Messina Abyssal Plain, *Initial Rep. Deep Sea Drill. Proj.*, *42*, 175–217.

Hubral, P. (1977), Time migration—Some ray theoretical aspects, *Geophys. Prospect.*, *25*, 738–745, doi:10.1111/j.1365-2478.1977.tb01200.x.

Jolivet, L., and C. Faccenna (2000), Mediterranean extension and the Africa-Eurasia collision, *Tectonics*, *19*, 1095–1106, doi:10.1029/2000TC900018.

Jongsma, D., J. E. van Hinte, and J. M. Woodside (1985), Geologic structure and neotectonics of the North African Continental Margin south of Sicily, *Mar. Pet. Geol.*, *2*, 156–179, doi:10.1016/0264-8172(85)90005-4.

Jongsma, D., J. M. Woodside, G. C. P. King, and J. E. van Hinte (1987), The Medina Wrench: A key to the kinematics of the central and eastern Mediterranean over the past 5 Ma, *Earth Planet. Sci. Lett.*, *82*, 87–106, doi:10.1016/0012-821X(87)90109-9.

Konstantinovskaya, E. A., L. B. Harris, J. Poulin, and M. I. Gennady (2007), Transfer zones and fault reactivation in inverted rift basins: Insights from physical modelling, *Tectonophysics*, *441*, 1–26, doi:10.1016/j.tecto.2007.06.002.

Koopman, A., A. Speksnijder, and W. T. Horsfield (1987), Sandbox model studies of inversion tectonics, *Tectonophysics*, *137*, 379–388, doi:10.1016/0040-1951(87)90329-5.

Lamarche, G., C. Basile, J. Mascle, and F. Sage (1997), The Côte d'Ivoire–Ghana transform margin: Sedimentary and tectonic structure from multichannel seismic data, *Geo Mar. Lett.*, *17*, 62–69, doi:10.1007/PL00007209.

Le Meur, D. (1997), Etude géophysique de la structure profonde et de la tectonique active de la partie occidentale de la Ride Méditerranéenne, 225 pp., Ph.D. thesis, Univ. Paris XI, Paris.

Lofi, J., and S. Berne (2008), Evidence for pre-Messinian submarine canyons on the Gulf of Lions slope (western Mediterranean), *Mar. Pet. Geol.*, *25*, 804–817, doi:10.1016/j.marpetgeo.2008.04.006.

Lofi, J., et al. (2005), Erosional processes and paleo-environmental changes in the western Gulf of Lions (SW France) during the Messinian Salinity Crisis, *Mar. Geol.*, *217*, 1–30, doi:10.1016/j.margeo.2005.02.014.

Lofi, J., et al. (2011a), Seismic atlas of the Messinian Salinity Crisis markers in the Mediterranean and Black Seas, 72 pp. and one CD, Comm. de la Carte Géol. du Monde, Paris.

Lofi, J., et al. (2011b), Refining our knowledge of the Messinian Salinity Crisis records in the offshore domain through multi-site seismic analysis, *Bull. Soc. Geol. Fr.*, *182*(2), 163–180, doi:10.2113/gssgfbull.2182.2112.2163.

Loubrieu, B., J. Mascle, and the Medipmap Group (2007), Morphobathymetry of the Mediterranean Sea, Int. Comm. for the Sci. Explor. of the Mediter. Sea, Monaco.

Makris, J., R. Nicolich, and W. Weigel (1986), A seismic study in the western Ionian Sea, *Ann. Geophys.*, *4*, 665–678.

Malinverno, A., and W. B. F. Ryan (1986), Extension in the Tyrrhenian Sea and shortening in the Apennines as result of arc migration driven by sinking of the lithosphere, *Tectonics*, *5*, 227–245, doi:10.1029/TC005i002p00227.

Mandal, N., and A. Chattopadhyay (1995), Modes of reverse reactivation of domino-type normal faults: Experimental and theoretical approach, *J. Struct. Geol.*, *17*, 1151–1163, doi:10.1016/0191-8141(95)00015-6.

Mascle, J., and C. Basile (1988), Marges continentales transformantes, *C. R. Acad. Sci., Ser. IIA Earth Planet. Sci.*, *326*, 827–838.

Minelli, L., and C. Faccenna (2010), Evolution of the Calabrian accretionary wedge (central Mediterranean), *Tectonics*, *29*, TC4004, doi:10.1029/2009TC002562.

Nicolich, R., M. Laigle, A. Hirn, L. Cernobori, and J. Gallart (2000), Crustal structure of the Ionian margin of Sicily: Etna volcano in the frame of regional evolution, *Tectonophysics*, *329*, 121–139, doi:10.1016/S0040-1951(00)00192-X.

Pasquale, V., M. Verdoya, and P. Chiozzi (2005), Thermal structure of the Ionian slab, *Pure Appl. Geophys.*, *162*, 967–986, doi:10.1007/s00024-004-2651-x.

Pondrelli, S., et al. (2006), The Italian CMT dataset from 1977 to the present, *Phys. Earth Planet. Inter.*, *159*, 286–303, doi:10.1016/j.pepi.2006.07.008.

Ranero, C. R., and E. Banda (1997), The crustal structure of the Canary Basin: Accretion processes at slow spreading ridge, *J. Geophys. Res.*, *102*(B5), 10,185–10,201, doi:10.1029/97JB00101.

Raulin, C., et al. (2011), Late Triassic–early Jurassic block tilting along E–W faults, in southern Tunisia: New interpretation of the Tebaga of Medenine, *J. Afr. Earth Sci.*, *61*, 94–104, doi:10.1016/j.jafrearsci.2011.05.007.

Reston, T. J., C. M. Krawczyk, and D. Klaeschen (1996), The S reflector west of Galicia (Spain): Evidence from prestack depth migration for detachment faulting during continental breakup, *J. Geophys. Res.*, *101*, 8075–8091, doi:10.1029/95JB03466.

Reston, T. J., R. Von Huene, T. Dickmann, D. Klaeschen, and H. Kopp (2002), Frontal accretion along the western Mediterranean Ridge: The effect of the Messinian evaporites on wedge mechanics and structural style, *Mar. Geol.*, *186*, 59–82, doi:10.1016/S0025-3227(02)00173-1.

Ricou, L. E. (1994), Tethys reconstructed: Plates continental fragments and their boundaries since 260 Ma from Central America to south-eastern Asia, *Geodin. Acta*, *7*, 169–218.

Robertson, A. H. F., P. D. Clift, P. J. Degnan, and G. Jones (1991), Paleogeographic and paleotectonic evolution of the eastern Mediterranean Neotethys, *Palaeogeogr. Palaeoclimatol. Palaeoecol.*, *87*, 289–343, doi:10.1016/0031-0182(91)90140-M.

Rosenbaum, G., G. S. Lister, and C. Duboz (2002), Reconstruction of the tectonic evolution of the western Mediterranean since the Oligocene, in *Reconstruction of the Evolution of the Alpine-Himalayan Orogen*, edited by G. Rosenbaum and G. S. Lister, *J. Virtual Explor.*, *8*, 107–126.

Ryan, W. B. F., M. B. Cita, and H. J. Hsü (1973), The origin of the Mediterranean evaporates, *Initial Rep. Deep Sea Drill. Proj.*, *13*, 1203–1231.

Sage, F., B. Pontoise, J. Mascle, and C. Basile (1997), Structure of oceanic crust adjacent to a transform margin segment: The Côte d'Ivoire-Ghana transform margin, *Geo Mar. Lett.*, *17*, 31–39, doi:10.1007/PL00007204.

Sallarès, V., et al. (2011), Seismic evidence for the presence of Jurassic oceanic crust in the central Gulf of Cadiz (SW Iberian margin), *Earth Planet. Sci. Lett.*, doi:10.1016/j.epsl.2011.09.003, in press.

Sandwell, D. T., and W. H. F. Smith (2009), Global marine gravity from retracked Geosat and ERS-1 altimetry: Ridge segmentation versus spreading rate, *J. Geophys. Res.*, *114*, B01411, doi:10.1029/2008JB006008.

Scandone, P., et al. (1981), Mesozoic and Cenozoic rocks from the Malta Escarpment (central Mediterranean), *Am. Assoc. Pet. Geol. Bull.*, *65*, 1299–1319.

Schettino, A., and E. Turco (2011), Tectonic history of the western Tethys since the Late Triassic, *Geol. Soc. Am. Bull.*, *123*, 89–105, doi:10.1130/B30064.30061.

Şengör, A. M. C. (1979), Mid-Mesozoic closure of Permo-Triassic Tethys and its implications, *Nature*, *279*, 590–593, doi:10.1038/279590a0.

Şengör, A. M. C., Y. Yılmaz, and O. Sungurlu (1984), Tectonics of the Mediterranean Cimmerides: Nature and evolution of the western termination of Palaeo-Tethys, *Geol. Soc. London Spec. Publ.*, *17*, 77–112.

Serpelloni, E., et al. (2007), Kinematics of the western Africa-Eurasia plate boundary from focal mechanisms and GPS data, *Geophys. J. Int.*, *169*, 1180–1200, doi:10.1111/j.1365-246X.2007.03367.x.

Sioni, S. (1996), Mer Ionienne et Apulie depuis l'ouverture de l'Océan Alpin, 241 pp., Ph.D. thesis, Univ. de Bretagne Occidentale, Brest, France.

Stampfli, G. M., and G. Borel (2004), The TRANSMED transects in space and time: Constraints on the paleotectonic evolution of the Mediterranean domain, in The TRANSMED Atlas: The Mediterranean Region From Crust to Mantle, vol. 1, edited by W. Cavazza et al., pp. 53–80, Springer, Berlin, doi:10.1007/978-3-642-18919-7_3.

Stampfli, G. M., J. Marcoux, and A. Baud (1991), Tethyan margins in space and time, *Palaeogeogr. Palaeoclimatol. Palaeoecol.*, *87*, 373–409, doi:10.1016/0031-0182(91)90142-E.

Sykes, L. R. (1967), Mechanism of earthquakes and nature of faulting on the mid-oceanic ridges, *J. Geophys. Res.*, *72*, 2131–2153, doi:10.1029/JZ072i008p02131.

Wessel, P., and W. H. F. Smith (1991), Free software helps map and display data, *Eos Trans. AGU*, *72*, 441, doi:10.1029/90EO00319.

White, R. S., D. MacKenzie, and R. K. O'Nions (1992), Oceanic crustal thickness from seismic measurements and rare earth elements inversions, *J. Geophys. Res.*, *97*, 19,683–19,715, doi:10.1029/92JB01749.

Yilmaz, O. (1987), *Seismic Data Processing*, 526 pp., Soc. of Explor. Geophys., Tulsa, Okla.

N. Chamot-Rooke, Laboratoire de Géologie, Ecole Normale Supérieure, 24 rue Lhomond, F-75231 Paris CEDEX 05, France. (rooke@mailhost.geologie.ens.fr)

F. Gallais, D. Graindorge, and M.-A. Gutscher, Domaines Océaniques, UMR 6538, Institut Universitaire Européen de la Mer, Université de Brest, CNRS, Place Nicolas Copernic, F-29280 Plouzané, France. (flora.gallais@univ-brest.fr; graindor@univ-brest.fr; gutscher@univ-brest.fr)

D. Klaeschen, Leibniz Institute of Marine Sciences at University of Kiel (IFM-GEOMAR), Wischhofstrasse 1-3, D-24148 Kiel, Germany. (dklaeschen@ifm-geomar.de)